Using the Nondivergent Wind to Diagnose Mesoscale Circulation Systems in Convection-Allowing Models

Thomas J. Galarneau, Jr.

NOAA/OAR National Severe Storms Laboratory, Norman, Oklahoma

Email: thomas.galarneau@noaa.gov *Web: https://inside.nssl.noaa.gov/tgalarneau/*

Acknowledgments: Dan Keyser and Lou Wicker

Introduction

- Mesoscale circulation systems modulate when and where deep, moist convection occurs
- Dynamical diagnosis of mesoscale ascent associated with these systems is an important component of the research and forecast process
- Continuing increases in resolution of operational NWP models are resulting in the improved representation of mesoscale circulation systems, but these increases also have resulted in noisier diagnostic signatures of mesoscale ascent
- We hypothesize that using the nondivergent wind ($\mathbf{V}_{nd}$) in place of the geostrophic wind ($\mathbf{V}_g$) in the alternative balance framework will produce cleaner diagnostic signatures of mesoscale ascent in convection-allowing operational models (CAMs)
- Substituting $\mathbf{V}_{nd}$ (ψ) for $\mathbf{V}_g$ (ϕ) is fully consistent with QG theory (Nielsen-Gammon and Gold 2008)
- Use of $\mathbf{V}_{nd}$ has been shown to improve diagnostic signatures of mesoscale ascent with snowbands in cold season cyclones in global NWP models (Galarneau and Keyser 2008; Kenyon et al. 2020)
- We will extend QG diagnosis to CAMs by comparing diagnostic signatures of mesoscale ascent using $\mathbf{V}_{nd}$ and $\mathbf{V}_g$ for two warm season convection cases

Data and Wind Definitions

- Operational High-Resolution Rapid Refresh (HRRR) analyses at 3-km grid spacing
- Poisson equation for streamfunction (ψ) and velocity potential (χ) are solved with homogeneous boundary conditions ($\psi = \chi = 0$)
- Wind definitions: $\boldsymbol{V}_{div} = \boldsymbol{\nabla}_{\boldsymbol{p}}\chi$, $\boldsymbol{V}_{rot} = \hat{k}\times\boldsymbol{\nabla}_{\boldsymbol{p}}\psi$, $\boldsymbol{V}_{nd} = \boldsymbol{V} - \boldsymbol{V}_{div}$, $\boldsymbol{V}_{g} = \frac{1}{f}\hat{k}\times\boldsymbol{\nabla}_{\boldsymbol{p}}\phi$
- Raymond (1988) high-order low-pass filter used to reduce small-scale motions (e.g., gravity wave signatures in geopotential field) but retain forcing from coherent mesoscale features

Diagnostic Equations

- Vector frontogenesis: $\boldsymbol{F} = \frac{d}{dt}\boldsymbol{\nabla}\theta = F_n\hat{\boldsymbol{n}} + F_s\hat{\boldsymbol{s}}$ (Keyser et al. 1988)
  - $F_n = \frac{1}{2}|\boldsymbol{\nabla}\theta|(D - E\cos 2\beta) = |\boldsymbol{\nabla}\theta|\frac{\partial v_n}{\partial n}$
  - $F_s = \frac{1}{2}|\boldsymbol{\nabla}\theta|(\zeta + E\sin 2\beta) = |\boldsymbol{\nabla}\theta|\frac{\partial v_n}{\partial s}$

$D = \frac{\partial u}{\partial x} + \frac{\partial v}{\partial y}$ $\quad \zeta = \frac{\partial v}{\partial x} - \frac{\partial u}{\partial y}$ $\quad E = \left(E_{sh}^2 + E_{st}^2\right)^{1/2}$ $\quad E_{sh} = \frac{\partial v}{\partial x} + \frac{\partial u}{\partial y}$ $\quad E_{st} = \frac{\partial u}{\partial x} - \frac{\partial v}{\partial y}$

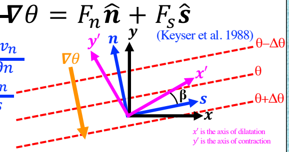

  - $\frac{d}{dt} = \frac{\partial}{\partial t} + \boldsymbol{V}_{nd}\cdot\boldsymbol{\nabla}$ in the alternative balance framework (Davies-Jones 1991; Keyser et al. 1992)
- F_n is the frontogenetical component and highlights banded vertical motion about baroclinic zones
- F_s is the rotational component and highlights cellular vertical motion associated with synoptic-scale waves
- **F** components in standard Cartesian coordinates are defined $\boldsymbol{F} = \left(-\frac{\partial \boldsymbol{V}_{nd}}{\partial x}\cdot\boldsymbol{\nabla}_{\boldsymbol{p}}\theta, -\frac{\partial \boldsymbol{V}_{nd}}{\partial y}\cdot\boldsymbol{\nabla}_{\boldsymbol{p}}\theta\right) = (F_1, F_2)$
- **Q** is the QG analog to **F**, where $\frac{d}{dt_g} = \frac{\partial}{\partial t} + \boldsymbol{V}_{\boldsymbol{g}}\cdot\boldsymbol{\nabla}$
- Omega equation: $\sigma\nabla_p^2\omega + f_0^2\frac{\partial^2\omega}{\partial p^2} = -2h(\boldsymbol{\nabla}_{\boldsymbol{p}}\cdot\boldsymbol{Q})$

Comparison of $\mathbf{V}_{nd}$/F and $\mathbf{V}_g$/Q for Supercell Case

MRMS Composite Reflectivity: 20 May 2019

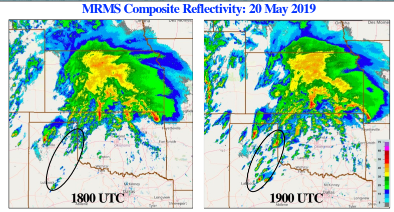

MRMS composite reflectivity (shaded in dBZ) at (left) 1800 and (right) 1900 UTC 20 May 2019. Source: https://mrms.nssl.noaa.gov/qvs/product_viewer/

- Dryline supercells initiate in TX Panhandle by 1900 UTC
- Filtered $\boldsymbol{\zeta}_g$ much noisier than filtered $\boldsymbol{\zeta}$

1800 UTC 20 May 2019

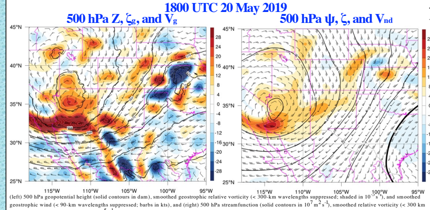

- Unfiltered $\mathbf{V}_{nd}$ smoother than filtered $\mathbf{V}_g$
- Filtered **Q** fields are noisy

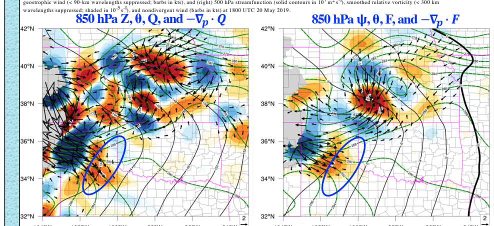

- Filtered **F** and $-\boldsymbol{\nabla}_{\boldsymbol{p}}\cdot\boldsymbol{F}$ fields are cleaner than **Q**, and mark ascent regions near dryline in TX and MCS in KS

Diagnostic Signatures of Ascent for MCS Case

MRMS Composite Reflectivity: 10 Aug 2020

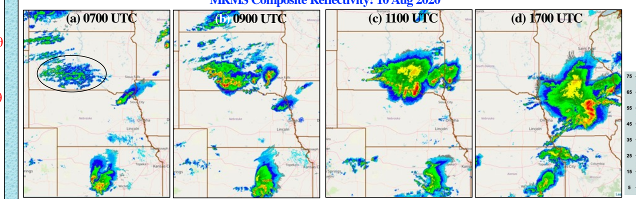

MRMS composite reflectivity (shaded in dBZ) at (a) 0700, (b) 0900, (c) 1100, and (d) 1700 UTC 10 Aug 2020. Source: https://mrms.nssl.noaa.gov/qvs/product_viewer/

0600 UTC 10 August 2020

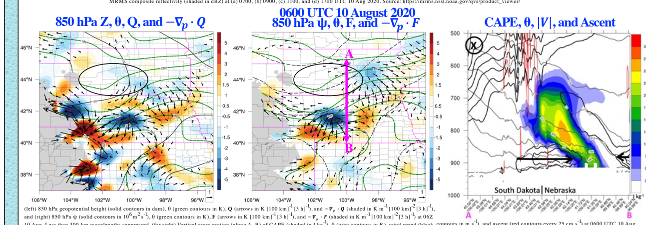

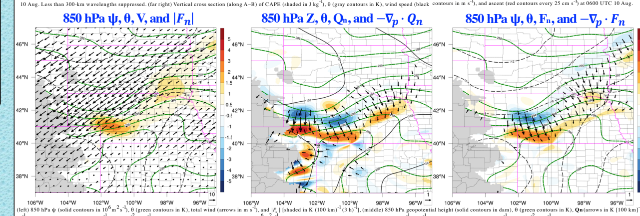

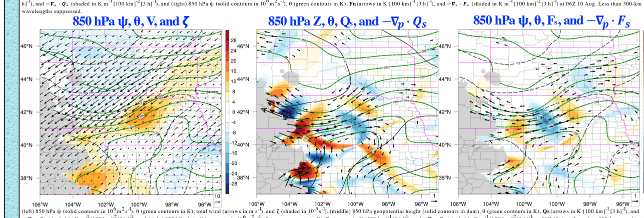

- Convection initiated north of a frontogenetical baroclinic zone and grew upscale to a derecho
- Filtered $\mathbf{F_n}$ and $-\boldsymbol{\nabla}_{\boldsymbol{p}}\cdot\boldsymbol{F_n}$ fields are cleaner than $\mathbf{Q_n}$, and show banded ascent forcing on warm side of front associated with frontogenesis

Conclusions

- Use of $\mathbf{V}_{nd}$ in the alternative balance framework produces cleaner and more coherent diagnostic signatures of mesoscale ascent and frontogenesis with less spatial smoothing than with $\mathbf{V}_g$